Novel Sampling Strategies for Sparse MR Image Reconstruction

Qiu Wang[1], Michael Zenge[2], Hasan Ertan Cetingul[1], Edgar Mueller[2], and Mariappan S Nadar[1]
[1]*Imaging and Computer Vision, Siemens Corporation, Corporate Technology, Princeton, NJ, United States,* [2]*MR Application & Workflow Development, Siemens AG, Healthcare Sector, Erlangen, Germany*

Introduction: Compressed sensing or sparsity-based MR reconstruction [1] takes advantage of the fact that the image is compressible in a specific transform domain, and enables reconstruction based on under-sampled *k*-space data thereby reducing the acquisition time. One requirement for the compressed sensing theory to work is the data acquisition in *k*-space to be incoherent. Although many random sampling schemes theoretically meet such requirements well enough, the MR physics or even the pathophysiology of a patient might impose additional constraints which have to be taken into account. This is considered the coherence barrier. In the current work, we formulate a sampling strategy that promises to achieve asymptotic incoherence, thus breaking the coherence barrier. Please notice that both the data acquisition and the reconstruction which have been used are investigational prototypes which experience continuous development. Nonetheless, experimental results in a phantom and a volunteer demonstrate a significant improvement of the spatial resolution with an increasing sub-sampling rate and a constant data acquisition time accordingly.

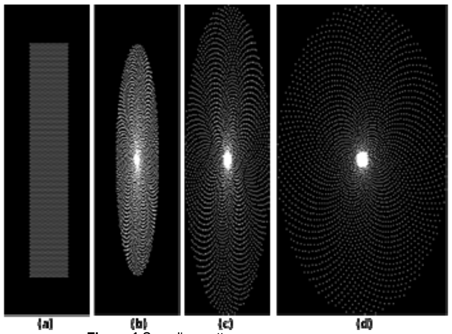
Figure 1 Sampling patterns

Methods: Although it is practically impossible to achieve perfect incoherence in almost all cases, recent publications [2, 3] indicate that it is possible to achieve asymptotic incoherence when the sampling size is large. This means an increase of the spatial resolution will yield substantially better results while keeping the total number of acquired lines in *k*-space constant.

<u>*Data acquisition*</u>: To prove this experimentally, a conventional gradient echo MR pulse sequence was modified to support different sampling patterns. MR acquisitions were performed on a clinical 1.5 T scanner (MAGNETOM Aera, Siemens AG, Healthcare Sector, Erlangen, Germany) in a phantom and a volunteer. Figure 1 plots the origin of frequency encoding lines of the patterns in the k_x-k_y phase encoding plane: (a) CAIPIRINHA [4] pattern with a total number of 2731 *k*-space lines as the standard of reference. Please notice a significant amount of zero padding in two directions. (b) Variable-density spiral phyllotaxis pattern [4] with 3139 sampled lines. The highest spatial frequencies were identical for (a) and (b). (c) The same sampling pattern with 3139 readouts redistributed to cover higher spatial frequencies. The reconstructed resolution was identical for (a) – (c). (d) Yet again, 3139 k-space lines, but increased spatial resolution in the partition dimension by a factor of two.

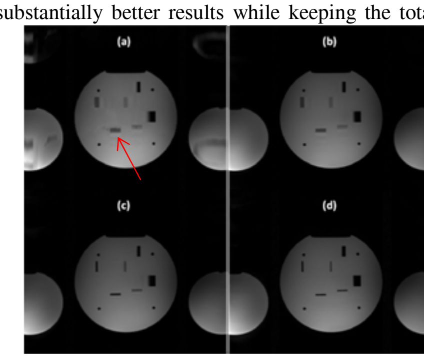
Figure 2 Phantom reconstructed from different sampling patterns

<u>*Image Reconstruction:*</u> In all experiments, the image reconstruction was performed and integrated at the MR scanner implementing the following equation [5]:

$$\min_x \frac{1}{2}\sum_{i=1}^{N_c}\left\|F_u(c_i \circ x) - y_i\right\|_2^2 + \lambda\left\|Wx\right\|_1$$

In this representation, x is a 1D vector which is the vectorized (concatenating columns vertically together) version of the signal to be reconstructed. N_c is the number of coils. F_u is the operator for image acquisition which includes Fourier transform and undersampling in *k*-space. c_i is the coil sensitivity profile for the i^{th} coil, and y is the acquired *k*-space data written in the vectorized form. $\circ$ is the element-wise multiplication. The regularization term is the L_1-norm of the signal in the wavelet transform domain, where W represents the redundant Haar wavelet transform.

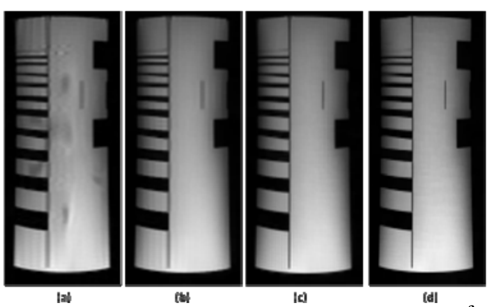
Figure 3 Reconstructed phantom viewed in the sagittal plane

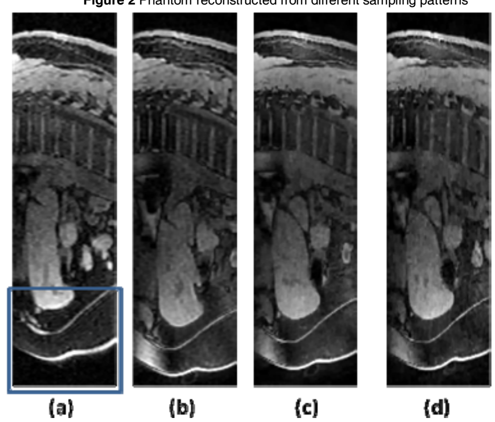
Figure 4 Reconstructed clinical 3D abdomen data viewed in the sagittal

Results: The overall image quality and spatial resolution of the different experiments was visually inspected. While subsampling artifacts were apparently avoided in all cases, significant differences in the spatial resolution can be observed. Figure 2 shows the results from the phantom data, displayed in the axial plane, comparing the four sampling patterns, respectively. The image resolution has been greatly improved from 2a (coherent sampling), 2b (basic incoherent sampling) to 2c and 2d (incoherent sampling with extended phase encoding measurements), especially around the thin rectangles marked by the red arrows. Figure 3 shows a sagittal reformation of the same data in the center of the object. In this orientation, the increase of the spatial resolution in the cases (c) and (d) is very obvious. Figure 4 represents the same results of the volunteer exam. Independent of the differences in the images due to different breath-hold positions, improvements in the spatial resolution can clearly be seen at tissue boundaries. This can even better be assessed in the magnified images of Figure 5.

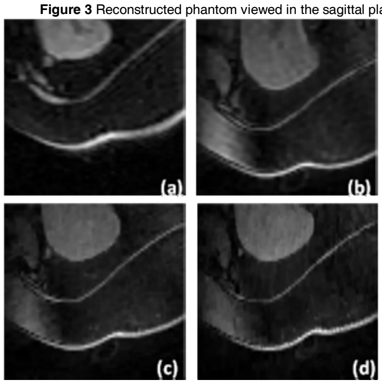
Figure 5 Enlarged views of the area highlighted in Figure 4

Discussion and Conclusion: Current results practically demonstrated that it is possible to break the coherence barrier by increasing the spatial resolution in MR acquisitions. This likewise implies that the full potential of the compressed sensing is unleashed only if asymptotic sparsity and asymptotic incoherence is achieved. Therefore, compressed sensing might better be used to increase the spatial resolution rather than accelerating the data acquisition in the context of non-dynamic 3D MR imaging.

References: [1] M. Lustig et al., Magnetic Resonance in Medicine, 2007. [2] B. Adcock et al., arXiv: 1302.0561, 2013. [3] F. Krahmer et al., arXiv :1210.2380v2, 2013. [4] FA Breuer et al., Magn Reson Med., Mar;55(3):549-56, 2006. [5] H. Vogel, Math. Biosci. 44, 179-189, 1979. [6] J. Liu et al., Proc Intl Soc Mag Reson Med, #4249, 2012.